Quantum suppression of the Rayleigh instability in nanowires

F Kassubek[1,2]**, C A Stafford**[2]**, Hermann Grabert**[1] **and Raymond E Goldstein**[2,3]

[1] Fakultät für Physik, Albert-Ludwigs-Universität, Hermann-Herder-Straße 3, D-79104 Freiburg, Germany
[2] Department of Physics, University of Arizona, Tucson, AZ 85721, USA
[3] Program in Applied Mathematics, University of Arizona, Tucson, AZ 85721, USA

Abstract
A linear stability analysis of metallic nanowires is performed in the free-electron model using quantum chaos techniques. It is found that the classical instability of a long wire under surface tension can be completely suppressed by electronic shell effects, leading to stable cylindrical configurations whose electrical conductance is a magic number $1, 3, 5, 6, \ldots$ times the quantum of conductance. Our results are quantitatively consistent with recent experiments with alkali metal nanowires.

AMS classification scheme numbers: 76E17, 81Q50, 82D35

PACS numbers: 4720D, 0545M, 6866L

1. Introduction

Plateau's celebrated study [1, 2] of the stability of bodies under the influence of surface tension established a fundamental result of classical continuum mechanics: a cylinder longer than its circumference is energetically unstable to breakup. Here we consider a quantum mechanical generalization of Plateau's study—the stability of a metallic nanowire. Methods from the study of quantum chaos [3, 4] are used to examine the energetics of a free-electron gas in a cylindrical jellium filament and show that an infinite filament can be stable against all axisymmetric perturbations if its electrical conductance G (in units of $G_0 = 2e^2/h = (12\,906.4 \text{ Ohm})^{-1}$) belongs to a set of 'magic numbers' $n = 1, 3, 5, 6, \ldots$ and is otherwise unstable. Here e is the charge of an electron and h is Planck's constant. Such magic numbers are analogous to those found in the shell model of atomic nuclei [4] and in metal clusters [4, 5]. Our stability analysis elucidates and confirms the stability properties of simple metal nanowires conjectured by Yanson *et al* [6] based on their observation of shell structure in the conductance statistics of sodium nanowires.
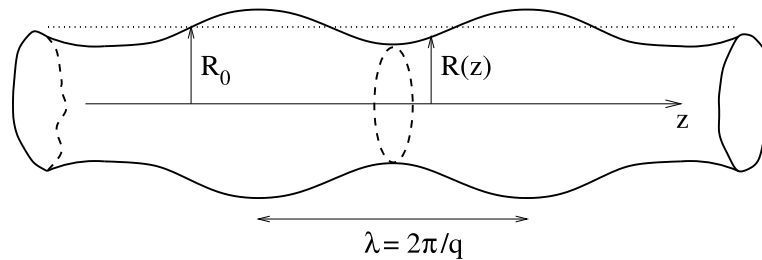
Figure 1. Deformation of wavevector q of a cylindrical nanowire.

Structural multistability of metallic nanowires was previously postulated based on classical molecular dynamics simulations [7–9]. However, the magic numbers observed in conductance histograms in alkali metals [6, 10] are clearly an electronic shell effect, as shown below, and cannot be explained with classical molecular dynamics. The common occurrence of multistability in two such radically different models likely stems from the fact that both models introduce an additional length scale (the Fermi wavelength λ_F in the free-electron model and the atomic diameter in molecular dynamics simulations), which leads to commensurability effects.

The properties of nanowires formed from simple monovalent metals, like the bulk properties of these materials [11], are determined largely by the delocalized conduction electrons. A free-electron jellium model, treating the electrons as a non-interacting Fermi gas confined within the wire by hard-wall boundary conditions, provides an intuitive and even quantitative explanation of observed quantities such as conductance [12–14], force [13–17] and shot noise [18]. To examine energetic stability, we consider a weakly deformed cylinder and find its thermodynamic potential to quadratic order in the amplitude of the deformation. A contribution proportional to the filament area, naturally identified as the surface tension, is only one of several competing terms in the free energy, which consists of terms which vary smoothly with the geometry of the filament and an oscillatory contribution directly connected with the discrete energy levels that are solutions to Schrödinger's equation. The smooth terms appear in descending powers of length (proportional to volume, surface area, mean curvature, etc) and are quite analogous to those found in the study of classical wave equations in curved domains [19] and the related problem of classically screened Coulomb (Debye–Hückel) interactions of curved surfaces in an electrolyte [20]. The oscillatory part of the free energy, in particular, alters Plateau's classical stability analysis in an essential way. This paper is thus fundamentally distinct from that which has dealt with the quantum mechanical origin of surface tension itself in metallic fluids [21], as well as those which consider quantum mechanical corrections to classical surface tension due to the quantization of capillary waves [22].

Long gold nanowires suspended between gold electrodes have been produced and imaged with a transmission–electron microscope by Kondo and Takayanagi [23, 24]; in particular, they have observed wires which are stable and almost perfectly cylindrical. The wires of [23, 24] are of finite length and attached to electrodes at either end. It seems reasonable to consider an infinite wire as a theoretical starting point and to assume that the length of the wire acts as a cut-off: deformations with a wavelength longer than the wire length cannot occur. Thus one does not have to model the boundary conditions at the ends of the wire, which would introduce additional parameters.

To be specific, we examine an infinite cylindrical wire and its sole classically unstable deformation—an axially symmetric one (see figure 1). Any such deformation can be written
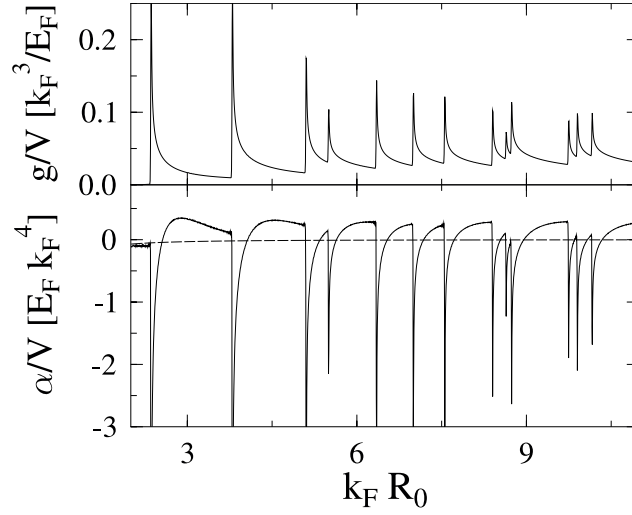
Figure 2. Density of states $g(E_F)$ of a cylindrical wire (upper diagram) and stability coefficient α (lower diagram) versus the radius R_0 of the unperturbed wire. The wavevector of the perturbation is $qR_0 = 1$. Broken curve, Weyl contribution to α.

as a Fourier series:

$$R(z) = R_0 \left(1 + \int_0^\infty dq\, b(q) \cos(qz + \phi(q))\right) \tag{1}$$

where $R(z)$ is the radius at position z, R_0 is the unperturbed radius, $b(q)$ is the (infinitesimal) perturbation coefficient and $\phi(q)$ is an arbitrary phase shift. The coefficients $b(q)$ are chosen such that the total volume of the wire is unchanged by the deformation. Other physically reasonable constraints [17] are also possible, but lead to similar results.

The metallic nanowire is an open system, connected to macroscopic metallic electrodes at each end [6, 10, 23–28]. Therefore, the change of the grand canonical potential Ω under the perturbation determines its stability. Ω is related to the electronic density of states $g(E)$ by

$$\Omega = -k_B T \int_0^\infty dE\, g(E) \ln\left(1 + e^{-(E-\mu)/k_B T}\right) \tag{2}$$

where k_B is Boltzmann's constant, T is the temperature and μ is the electronic chemical potential specified by the macroscopic electrodes. Our aim is to expand Ω up to second order in the coefficients $b(q)$ characterizing the deformation. As we will show, this yields

$$\Omega[b] = \Omega[0] + \int_0^\infty dq\, \alpha(q)[b(q)]^2 + \mathcal{O}(b^3). \tag{3}$$

The change in the grand canonical potential is of second order in b and contributions from deformations with different q decouple. If the prefactor $\alpha(q)$ is negative for any value of q, then Ω decreases under the deformation and the wire is unstable.

For an infinite cylindrical wire, the transverse motion is quantized, leading to the formation of discrete electronic subbands. The total density of states is the sum of the contributions from each subband (see figure 2): every subband begins to contribute at a threshold energy equal to the energy of its quantized transverse motion with a sharp spike, falling off smoothly for increasing energy. If the Fermi energy E_F lies near one of these sharp peaks, certain small

deformations of the wire can dramatically increase the density of states. According to (2), this lowers the grand canonical potential, leading to an instability. On the other hand, if there is no subband threshold sufficiently close to E_F, the density of states will instead decrease with any deformation, implying the existence of stable regions in the intervals between the instabilities associated with the opening of each subband.

2. Quantum chaos approach

In order to examine this picture quantitatively, we use a semiclassical approach [3, 4], which enables $g(E)$ to be split into a smooth average contribution $\bar{g}(E)$, referred to as the *Weyl contribution* and an oscillatory part $\delta g(E)$, whose average value is zero:

$$g(E) = \bar{g}(E) + \delta g(E). \tag{4}$$

The Weyl term $\bar{g}$ contains terms proportional to the volume of the nanowire and to the area and curvature of its surface: $\bar{g}(E) = (1/E_F)\tilde{g}(E/E_F)$, where

$$\tilde{g}(x) = \frac{x^{1/2}}{2\pi^2}k_F^3 V - \frac{1}{8\pi}k_F^2 S + \frac{x^{-1/2}}{6\pi^2}k_F K \tag{5}$$

and $k_F = 2\pi/\lambda_F$ is the Fermi wavevector. The volume V, surface area S and integrated mean curvature K can be calculated for arbitrary perturbations by simple geometric considerations. The oscillatory part δg of the density of states is a quantum correction and may be calculated in the semiclassical approximation as a sum over all periodic classical orbits of the system [3, 4, 16, 17, 29–31].
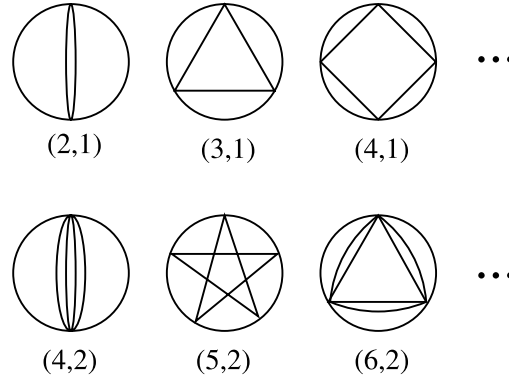

Figure 3. Classical periodic orbits of an electron in a plane perpendicular to the z-axis, labelled (v, w), where v is the number of vertices and w the winding number.

Let us first consider an undeformed cylindrical wire. Each periodic orbit lies in a plane transverse to the wire's axis and there is a correspondence to the orbits [4] in a circular billiard (see figure 3). Note that the action S_{vw} of each orbit is invariant under both translations of the orbit parallel to the z-axis and rotations about the z-axis. In a system with continuous symmetries, when taking the trace of the electron Green's function to calculate the density of states, one must first integrate exactly over these symmetries [4, 29] before employing the semiclassical (stationary phase) approximation. For electrons in a cylinder of length L, one obtains the following trace formula:

$$\delta g(E) = \frac{mL}{\pi\hbar^2} \sum_{w=1}^{\infty} \sum_{v=2w}^{\infty} \frac{f_{vw}L_{vw}}{v^2} \cos\left(\frac{S_{vw}(E)}{\hbar} - \frac{3v\pi}{2}\right) \tag{6}$$

where m is the electron mass, v and w are defined in figure 3, $f_{vw} = 1 + \theta(v - 2w)$ counts the discrete degeneracy of the orbit under time reversal, $L_{vw} = 2vR_0 \sin(\pi w/v)$ is the length of a periodic orbit and the action $S_{vw}/\hbar = k_F L_{vw} \sqrt{E/E_F}$.

When the wire is deformed, the translational symmetry is broken and we use a semiclassical perturbation theory [30, 31] to calculate δg. This theory assumes that for small perturbations, the amplitudes and topology of the unperturbed orbits can still be used in (6), but that the lengths of the orbits—and hence their actions—change. The trace formula becomes

$$\delta g(E) = \frac{m}{\pi \hbar^2} \sum_{w=1}^{\infty} \sum_{v=2w}^{\infty} \frac{f_{vw}}{v^2} \operatorname{Re} \left\{ e^{i(S_{vw}/\hbar - 3v\pi/2)} \int_0^L dz \, (L_{vw} + \Delta L_{vw}) \, e^{i \Delta S_{vw}/\hbar} \right\} \tag{7}$$

where $\Delta S_{vw}/\hbar = k_F \Delta L_{vw} \sqrt{E/E_F}$ and

$$\Delta L_{vw} = 2v \sin(\pi w/v)(R(z) - R_0) \tag{8}$$

which may be expressed in terms of the perturbation coefficients using equation (1). Combining this result for δg with (5), it is straightforward to calculate the density of states up to second order in the coefficients $b(q)$ for a deformed wire. The result can be integrated to obtain the grand canonical potential, which indeed has the expansion (3).

3. Stability analysis

Let us first discuss the stability of a nanowire at zero temperature. Figure 2 shows the stability coefficient α (lower diagram) and the density of states at the Fermi energy (upper diagram) as functions of the radius of the unperturbed wire. The wavelength of the perturbation was taken to be $qR_0 = 1$, the critical wavelength for stability in Plateau's classical analysis of a body under the influence of surface tension. In addition to surface tension, the present model for Ω has a curvature energy, which enhances the instability for small R_0 and an oscillatory component associated with the opening of successive subbands as R_0 increases. As discussed above, α has sharp negative peaks—indicating strong instabilities—at the subband thresholds, where the density of states is sharply peaked. Under surface tension and curvature energy alone (broken curve in figure 2), the wire would be slightly unstable at the critical wavevector $qR_0 = 1$, since the curvature term is negative. However, the quantum correction is positive in the regions between the thresholds to open new subbands, *thus stabilizing the wire*. Since the oscillatory contribution to α is independent of q, we find that regions of stability persist for *arbitrarily long wavelength perturbations*, indicating that an infinitely long cylindrical wire is a true metastable state if the radius lies in one of the windows of stability.

With these results, we can construct the zero-temperature stability diagram for the wire (see figure 4(a)). In contrast to Plateau's classical stability analysis, an additional quantum length scale arises here, namely the Fermi wavelength λ_F. The stability problem is now determined by two dimensionless parameters: qR_0 and $k_F R_0$. In figure 4, regions of instability, where the coefficient $\alpha(q)$ is negative, are shaded grey, while the stable regions are shown in white. Note that many of the white regions of stability persist all the way down to $q = 0$. The *multistability* of the system, indicated by the alternating stable and unstable stripes, reflects commensurability effects between λ_F and R_0.

We note that in addition to the axially symmetric modes considered here, which are the sole unstable modes in the classical limit, perturbations which break axial symmetry may also become unstable near the subband thresholds. However, these Jahn–Teller-like modes [15] are likely to be less unstable than the axisymmetric modes and will not destroy the regions of stability shown in figure 4(a).
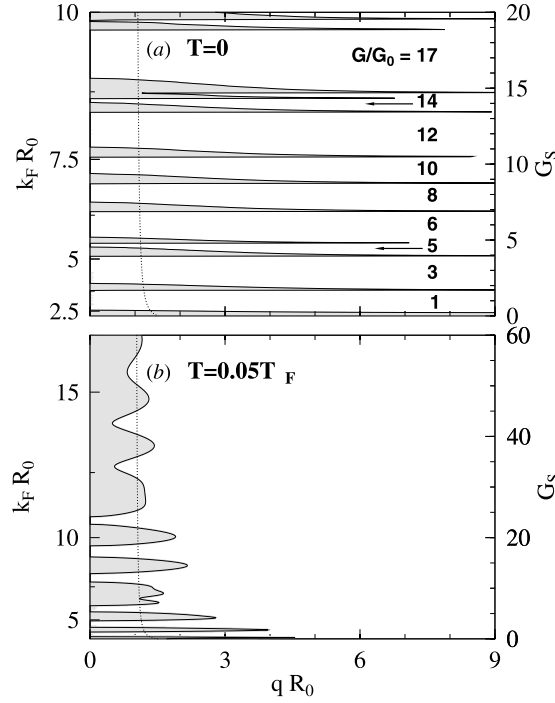
Figure 4. Stability diagram for cylindrical nanowires at two different temperatures. White areas are stable, grey unstable to small perturbations. The quantized electrical conductance values G of the stable configurations are indicated by bold numerals in (*a*), with $G_0 = 2e^2/h$. Right vertical axis, corrected Sharvin conductance G_S. Dotted curve, stability criterion in the Weyl approximation.

4. Conductance magic numbers

The electrical conductance G of a perfect cylindrical nanowire is quantized [12] in units of $G_0 = 2e^2/h$. The quantized conductance values of the stable cylindrical configurations are indicated by bold numerals in figure 4(*a*). For comparison, the right vertical axis of the figure is labelled with the corrected Sharvin conductance [12]

$$G_S = \left(\frac{k_F R_0}{2}\right)^2 \left(1 - \frac{2}{k_F R_0}\right) \tag{9}$$

which gives a smooth approximation to G/G_0. The conductance values of the stable configurations are somewhat analogous to the *magic numbers* of enhanced stability in atomic nuclei [4] and metal clusters [4, 5]. An important distinction is that the magic numbers in nuclei and clusters refer to the number of fermions in a finite system, while we consider an infinite, open system, with magic numbers describing the number of conducting transverse modes [13] which hold the wire together. The number of conducting modes is approximately equal to the number of atoms which fit within a cross section of the wire.

The integer magic numbers identified here must be distinguished from the concept of 'magic wire configurations' proposed by van Ruitenbeek and others [15, 32, 33]. The latter represented discrete minima of the energy per unit volume of a jellium wire as a function of its cross sectional area, but the stability with respect to deformations with $q > 0$ was not considered. A similar scenario was advanced in [6] based on a partial summation of the periodic orbits in the expression for Ω itself. While the theoretical results of [6, 15, 32, 33]

seem to imply that stability occurs only for a discrete set of radii, of measure zero, our analysis finds stability with respect to small perturbations over broad intervals of radius. Furthermore, the very existence of discrete energetic minima of the type discussed in [6, 15, 32, 33] depends sensitively on the numerical value of the surface tension in the model; for example, they do not occur whatsoever in the free-electron model at constant volume for $G > G_0$. In contrast, the finite windows of stability in our analysis are robust with respect to variations of the surface tension.

5. Comparison with experiments in alkali metals

The sequence of magic numbers $G/G_0 = 1, 3, 5, 6, \ldots$ is consistent with the observation of conductance quantization in alkali metal point contacts [10]. Recently, conductance histograms for sodium nanowires with pronounced peaks up to $G/G_0 \sim 100$ were obtained by Yanson *et al* [6]. They argued that these peaks could not be understood based on conductance quantization alone, but rather reflected energetically preferred wire configurations. In order to construct a theoretical conductance histogram, we need to know the *a priori probability* of occurrence of a nanowire of a given cross sectional area. Here, we make the simplest hypothesis: that *nanowires of different cross sectional areas occur with equal a priori probability if stable and with zero probability otherwise*. On this hypothesis, the relative probability of observing a contact with a given quantized conductance value is proportional to the width ΔG_S of the corresponding stable region, G_S being a dimensionless measure of the contact area.

The conductance histogram from [6] taken at a temperature of $T = 80$ K is reproduced in our figure 5(a). For comparison, the theoretical magic numbers at the same temperature are plotted as vertical bars, with height equal to the width ΔG_S of the corresponding stable region. Unlike the idealized wires in our analysis, the experimental wires are of finite length and contain imperfections. Thus the peaks in the experimental histogram are shifted [14] below the theoretical integer values due to backscattering and are broadened [14] due to tunnelling, disorder-induced conductance fluctuations and inelastic processes. Furthermore, the relative heights of the peaks may be influenced by dynamical as well as energetic effects; in particular, the peak at $G = G_0$, which is quite pronounced at the lowest temperatures [6, 10], is absent from the experimental histogram at $T = 80$ K—presumably indicating that thermally activated processes lead to the rupture of this metastable configuration.

While the first four theoretical peaks at $G/G_0 = 1, 3, 5, 6$ can be identified unambiguously with the narrower peaks in the low-temperature data of [6, 10], it is not entirely clear whether one can match up the broad peaks in the 80 K experimental histogram with individual theoretical magic numbers. In particular, there appears to be fine structure in the theoretical histogram which is not present in the 80 K histogram, possibly because it is obscured due to broadening. In order to see whether the theoretical histogram nonetheless correctly describes the gross features of the experimental histogram, it is useful to take the Fourier transforms of the two histograms, singling out the contributions of the shortest periodic orbits.

The actions of the periodic orbits are proportional to the radius of the wire and hence are approximately proportional to the square root of the conductance, by equation (9). The contributions of the various periodic orbits to the conductance histogram can thus be extracted [34] by taking a Fourier transform with respect to $\sqrt{G/G_0}$. The Fourier power spectrum of the theoretical conductance histogram is shown as a full curve in figure 5(b), where all magic numbers up to $G/G_0 = 207$ were included. It shows clear peaks corresponding to the three shortest periodic orbits. For comparison, the experimental Fourier spectrum for sodium nanowires at 90 K obtained by Yanson *et al* [34] is shown as a broken curve. The experimental spectrum contains two broad peaks, one centred at the frequency of the diameter orbit and
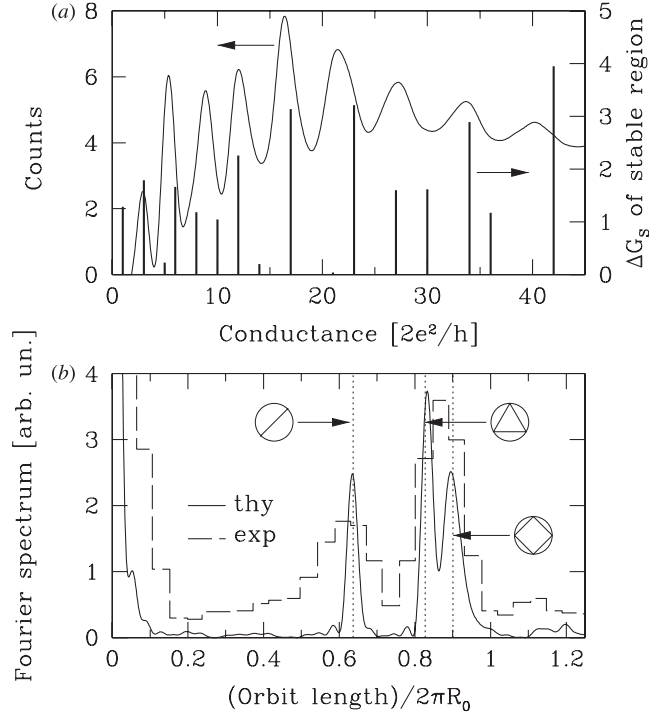
Figure 5. Magic numbers: theory and experiment. (*a*) Full curve, conductance histogram for sodium nanowires at $T = 80$ K $= 0.002T_F$, reproduced from [6]. Vertical bars, quantized conductance values of the metastable nanowire configurations in the free-electron model at the same temperature. The height of each bar is equal to the width ΔG_S of the corresponding stable region (cf figure 4(*a*)). (*b*) Full curve, Fourier power spectrum of the theoretical conductance histogram (vertical bars in (*a*)), displaying the dominant contributions of the three shortest periodic orbits in equation (7). Broken curve, Fourier power spectrum of the conductance histogram for sodium nanowires at $T = 90$ K, reproduced from [34]. Note that the theoretical Fourier spectrum does not change significantly between 80 and 90 K.

a second which spans the frequencies of the triangle and square orbits. The experimental peaks in figure 5(*b*) are broader than the theoretical peaks since the oscillatory structure in the experimental histogram is damped for $G/G_0 > 50$. The widths of the theoretical peaks, in contrast, are determined by the maximum conductance included, $\max\{G/G_0\} = 207$; increasing this cut-off decreases the widths of the peaks. We have simply taken a cut-off larger than the maximum measured conductance, so that the cut-off does not introduce any artefacts in the theoretical Fourier spectrum. The overall vertical scale of the power spectra shown is arbitrary, so a comparison between theory and experiment must be based on the relative spectral weights of the various peaks. In both spectra, the weight of the diameter orbit is roughly half the combined spectral weights of the triangle and square orbits—a rather good agreement between theory and experiment.

6. Classical limit

At zero temperature, the pattern of stable regions separated by unstable stripes shown in figure 4(*a*) continues up to arbitrarily large radii. However, at any finite temperature T, the

quantum oscillations in α are smoothed out and the classical stability criterion $qR_0 > 1$ is recovered asymptotically for sufficiently large radii. The crossover from the $T = 0$ result to the classical limit occurs when $k_B T \sim E_F(G_0/G)$, i.e. when the thermal energy $k_B T$ is comparable to the average transverse level spacing. Figure 4(b) shows the stability diagram for $T/T_F = 0.05$, where $T_F = E_F/k_B$ is the Fermi temperature. One sees that the stability boundary indeed begins to cross over to the classical line $qR_0 = 1$ for $G_S > 20$.

In figure 4(b), there are no true metastable configurations with $G_S > 25 \sim T_F/T$, indicating that all thicker wires would be dynamically unstable (like a column of fluid) at this temperature, once the electronic shell effects have been smoothed out. However, $T_F = 3.75 \times 10^4$ K in sodium, so multistability from electronic shell effects can be expected to occur in sodium contacts with $G/G_0 \lesssim 125$ up to at least 300 K.

7. Discussion

It should be pointed out that thermal averaging is not the only mechanism that can suppress electronic shell effects. Disorder also tends to smooth out the sharply peaked structure in the density of states, so that one can expect a reduction of shell effects when the diameter of the wire exceeds the mean free path. Furthermore, the tendency of the positive ions to order themselves into regular arrays [23, 24] will certainly affect the stability of metallic nanowires. Indeed, pioneering theoretical investigations [7–9] of the dynamics of nanowires focused exclusively on the arrangement of the ions. Based on the relative importance of electronic shells and crystal structure in metal clusters [5], one would expect electronic shell effects to dominate the energetics of very thin wires, particularly in the alkali metals, with crystal structure becoming increasingly important for thicker wires and for metals where the bonding is more directional.

Although conductance histograms of gold nanowires [26] do not exhibit the sequence of magic numbers predicted here and observed in alkali metals, there is some evidence that gold nanowires can otherwise be adequately described using the free-electron model [13, 14, 18]. It is thus worthwhile to speculate about a possible electronic origin for the remarkable stability of wires of individual gold atoms. Linear chains composed of four to seven gold atoms suspended between two gold electrodes, with a conductance $G = G_0$, were found to be stable in the laboratory for hours at a time [27, 28]. Given that such a configuration has an enormous surface energy, its stability is at first sight surprising. However, in our free-electron model, we find that an infinitely long wire with a conductance of G_0 is indeed stable with respect to small perturbations.

Our results may also be relevant to explain the observed stability of gold wires with larger radii [23, 24]. The atomic-scale structure of these wires exhibits a remarkable diversity, ranging from helical, multishell structures [24] to crystalline structures with surface reconstruction [23]; but a common factor in the observed stable structures is that they are almost perfectly cylindrical. A direct comparison to our theoretical stability analysis would be facilitated by measurements of the conductance of the stable wires, which have not yet been carried out. However, a rule of thumb is that the conductance G/G_0 of a metal wire made of monovalent atoms is roughly equal to the number of atoms in the cross section. Thus the hexagonal prism structure with a cross section of 30 atoms determined in [23] does correspond to a stable configuration in our analysis (vertical bar at $G/G_0 = 30$ in figure 5(a)). Similarly, the thinnest of the helical wire structures determined in [24], with a cross section of eight atoms, also corresponds to a stable structure in our analysis, while the two thickest wire structures determined in [24], with cross sections of 22 and 24 atoms, respectively, appear to straddle the predicted island of stability at $G/G_0 = 23$. Further work is needed to elucidate the interplay of atomistic stacking effects and electronic shell effects in these structures.

Finally, let us comment on the dynamical evolution of a nanowire under elongation or compression. Consider stretching a nanowire that is initially in a stable configuration (white areas in figure 4). Under elongation, the radius of the wire decreases, so that one moves downward on the stability diagram. When a stability boundary is encountered, it becomes energetically (and dynamically) favourable for the wire to deform spontaneously, until another stable configuration of smaller radius is reached, thus causing the conductance to jump abruptly from one magic number to a smaller one and conversely under compression. This scenario is consistent with the claim [25] that the structure of a metallic nanowire undergoes a sequence of abrupt changes as a function of elongation or compression. The finite widths of the unstable tongues in figure 4 also provides a possible explanation for the hysteresis [25] observed in the conductance as a function of elongation: the critical radius at which the wire's conductance jumps between neighbouring magic numbers is different, depending on whether the tongue is approached from above or below, i.e. depending on whether the wire is stretched or compressed.

Acknowledgments

References

[1] Plateau J 1873 *Statique Expérimentale et Théorique des Liquides Soumis aux Seules Forces Moléculaires* (Paris: Gauthier-Villars)
[2] Chandrasekhar S 1981 *Hydrodynamic and Hydromagnetic Stability* (New York: Dover) pp 515–74
[3] Gutzwiller M C 1990 *Chaos in Classical and Quantum Mechanics* (New York: Springer)
[4] Brack M and Bhaduri R K 1997 *Semiclassical Physics* (Reading, MA: Addison-Wesley)
[5] de Heer W A 1993 The physics of simple metal clusters: experimental aspects and simple models *Rev. Mod. Phys.* **65** 611–76
[6] Yanson A I, Yanson I K and van Ruitenbeek J M 1999 Observation of shell structure in sodium nanowires *Nature* **400** 144–6
[7] Landman U, Luedtke W D, Burnham N A and Colton R J 1990 Atomistic mechanisms and dynamics of adhesion, nanoindentation and fracture *Science* **248** 454–61
[8] Todorov T N and Sutton A P 1993 Jumps in electronic conductance due to mechanical instabilities *Phys. Rev. Lett.* **70** 2138–41
[9] Sørensen M R, Brandbyge M and Jacobsen K W 1998 Mechanical deformation of atomic-scale metallic contacts: structure and mechanisms *Phys. Rev.* B **57** 3283–94
[10] Krans J M, van Ruitenbeek J M, Fisun V V, Yanson I K and de Jongh L J 1995 The signature of conductance quantization in metallic point contacts *Nature* **375** 767–9
[11] Ashcroft N W and Mermin N D 1976 *Solid State Physics* (New York: Saunders College Publishing) pp 29–55
[12] Torres J A, Pascual J I and Sáenz J J 1994 Theory of conduction through narrow constrictions in a three-dimensional electron gas *Phys. Rev.* B **49** 16581–4
[13] Stafford C A, Baeriswyl D and Bürki J 1997 Jellium model of metallic nanocohesion *Phys. Rev. Lett.* **79** 2863–6
[14] Bürki J, Stafford C A, Zotos X and Baeriswyl D 1999 Cohesion and conductance of disordered metallic point contacts *Phys. Rev.* B **60** 5000–8
[15] van Ruitenbeek J M, Devoret M H, Esteve D and Urbina C 1997 Conductance quantization in metals: the influence of subband formation on the relative stability of specific contact diameters *Phys. Rev.* B **56** 12 566–72
[16] Höppler C and Zwerger W 1999 Quantum fluctuations in the cohesive force of metallic nanowires *Phys. Rev.* B **59** R7849–51

[17] Stafford C A, Kassubek F, Bürki J and Grabert H 1999 Universality in metallic nanocohesion: a quantum chaos approach *Phys. Rev. Lett.* **83** 4836–9

[18] Bürki J and Stafford C A 1999 Comment on quantum suppression of shot noise in atom-size metallic contacts *Phys. Rev. Lett.* **83** 3342

[19] Balian R and Bloch C 1970 Distribution of eigenfrequencies for the wave equation in a finite domain I: 3D problem with a smooth boundary surface *Ann. Phys., NY* **60** 401–47

[20] Duplantier B, Goldstein R E, Romero-Rochín V and Pesci A I 1990 Geometrical and topological aspects of electric double layers near curved surfaces *Phys. Rev. Lett.* **65** 508–11

[21] d'Evelyn M P and Rice S A 1983 Pseudoatom theory for the liquid–vapor interface of a simple metal: computer simulation studies of sodium and cesium *J. Chem. Phys.* **78** 5225–49

[22] Ebner C and Saam W F 1975 Renormalized density-functional theory of nonuniform superfluid ^{4}He at zero temperature *Phys. Rev.* B **12** 923–39

[23] Kondo Y and Takayanagi K 1997 Gold nanobridge stabilized by surface structure *Phys. Rev. Lett.* **79** 3455–8

[24] Kondo Y and Takayanagi K 2000 Synthesis and characterization of helical multi-shell gold nanowires *Science* **289** 606–8

[25] Rubio G, Agraït N and Vieira S 1996 Atomic-sized metallic contacts: mechanical properties and electronic transport *Phys. Rev. Lett.* **76** 2302–5

[26] Costa-Krämer J L, García N and Olin H 1997 Conductance quantization histograms of gold nanowires at 4 K *Phys. Rev.* B **55** 12 910–13

[27] Ohnishi H, Kondo Y and Takayanagi K 1999 Quantized conductance through individual rows of suspended gold atoms *Nature* **395** 780–3

[28] Yanson A I, Rubio Bollinger G, van den Brom H E, Agraït N and van Ruitenbeek J M 1999 Formation and manipulation of a metallic wire of single gold atoms *Nature* **395** 783–5

[29] Creagh S C and Littlejohn R G 1991 Semiclassical trace formulas in the presence of continuous symmetries *Phys. Rev.* A **44** 836–50

[30] Ullmo D, Grinberg M and Tomsovic S 1996 Near-integrable systems: resonances and semiclassical trace formulas *Phys. Rev.* E **54** 136–52

[31] Creagh S C 1996 Trace formula for broken symmetry *Ann. Phys., NY* **248** 60–94

[32] Yannouleas C and Landman U 1997 On mesoscopic forces and quantized conductance in model metallic nanowires *J. Phys. Chem.* B **101** 5780–3

[33] Zabala N, Puska M J and Nieminen R M 1999 Electronic structure of cylindrical simple-metal nanowires in the stabilized jellium model *Phys. Rev.* B **59** 12 652–60

[34] Yanson A I, Yanson I K and van Ruitenbeek J M 2000 Supershell structure in alkali metal nanowires *Phys. Rev. Lett.* **84** 5832–5